The American Journal of Pathology, Vol. 193, No. 1, January 2023

ELSEVIER

The American Journal of PATHOLOGY

ajp.amjpathol.org

BIOMARKERS, GENOMICS, PROTEOMICS, AND GENE REGULATION

Genomic Characterization of Prostatic Basal Cell Carcinoma

Jin-Yih Low,[*] Minjeong Ko,[†] Brian Hanratty,[*] Radhika A. Patel,[*] Akshay Bhamidipati,[‡] Christopher M. Heaphy,[‡§¶] Erolcan Sayar,[*] John K. Lee,[*‖] Shan Li,[*] Angelo M. De Marzo,[‡§**] William G. Nelson,[‡§**] Anuj Gupta,[‡] Srinivasan Yegnasubramanian,[‡§] Gavin Ha,[*†] Jonathan I. Epstein,[‡§**] and Michael C. Haffner[*‡§‖††]

From the Divisions of Human Biology,[*] Public Health Science,[†] and Clinical Research,[‖] Fred Hutchinson Cancer Center, Seattle, Washington; Sidney Kimmel Comprehensive Cancer Center,[‡] Department of Pathology,[§] and Department of Urology,[**] James Buchanan Brady Urological Institute, Johns Hopkins University School of Medicine, Baltimore, Maryland; Department of Medicine,[¶] Boston University School of Medicine and Boston Medical Center, Boston, Massachusetts; and the Department of Laboratory Medicine and Pathology,[††] University of Washington, Seattle, Washington

Accepted for publication September 30, 2022.

Address correspondence to Jonathan I. Epstein, M.D., Department of Pathology, The Johns Hopkins Hospital, 401 N. Broadway, Baltimore, MD 21231; or Michael C. Haffner, M.D., Ph.D., Division of Human Biology, Fred Hutchinson Cancer Center, 1100 Fairview Ave., Seattle, WA 98109.
E-mail: jepstein@jhmi.edu or mhaffner@fredhutch.org.

Basal cell carcinoma (BCC) of the prostate is a rare tumor. Compared with the more common acinar adenocarcinoma (AAC) of the prostate, BCCs show features of basal cell differentiation and are thought to be biologically distinct from AAC. The spectrum of molecular alterations of BCC has not been comprehensively described, and genomic studies are lacking. Herein, whole genome sequencing was performed on archival formalin-fixed, paraffin-embedded specimens of two cases with BCC. Prostatic BCCs were characterized by an overall low copy number and mutational burden. Recurrent copy number loss of chromosome 16 was observed. In addition, putative driver gene alterations in *KIT*, *DENND3*, *PTPRU*, *MGA*, and *CYLD* were identified. Mechanistically, depletion of the CYLD protein resulted in increased proliferation of prostatic basal cells *in vitro*. Collectively, these studies show that prostatic BCC displays distinct genomic alterations from AAC and highlight a potential role for loss of chromosome 16 in the pathogenesis of this rare tumor type. *(Am J Pathol 2023, 193: 4–10; https://doi.org/10.1016/j.ajpath.2022.09.010)*

The prostate is lined by a bilayered epithelium composed of basal cell and luminal cell layers.[1] Most prostate cancers show features of prostatic luminal cell differentiation and demonstrate an acinar growth pattern.[2] However, a distinct subtype of prostatic carcinomas shows morphologic and molecular similarities with prostatic basal cells, and is termed prostatic basal cell carcinoma (BCC).[3–6] Prostatic BCCs are extremely rare tumors, with only several dozen cases described in the literature.[3–5,7,8]

Although most BCCs are considered indolent, recent studies showed that more than 40% of patients experience disease recurrence after initial therapy. In addition,

Supported by NIH National Cancer Institute grants P50CA097186, R01 CA234715, U54CA224079, P30CA015704 P30CA006973, PO1CA163227, P50CA58236, and K22 CA237746) NIH Office of Research Infrastructure Programs grant S10OD028685, US Department of Defense Prostate Cancer Research Program grants W81XWH-20-1-0111, W81XWH-21-1-0229, W81XWH-18-1-0347 W81XWH-18-1-0756, PC170510; W81XWH-18-1-0356, PC170503P2, and PC200262P1, Doris Duke Charitable Foundation grant 2021184, the Prostate Cancer Foundation, the Safeway Foundation, the Richard M. Lucas Foundation, the Fred Hutchinson Cancer Center/University of Washington Cancer Consortium, the Brotman Baty Institute for Precision Medicine and the University of Washington/Fred Hutchinson Cancer Center Institute for Prostate Cancer Research.

Disclosures: A.M.D.M. and S.Y. serve as consultants for Cepheid Inc. and receive sponsored research funding from Janssen R&D Inc. S.Y. receives sponsored research funding from Cepheid Inc. A.M.D.M. serves as a consultant to Merck Inc. W.G.N. has been a member of the Cancer Scientific Advisory Council, AbbVie Inc., the Scientific Advisory Board, ProQuest Investments Inc., the Board of Directors, Armis Biopharma Inc., and the Scientific Advisory Board, Cepheid Inc.; is a cofounder and adviser for Digital Harmonics and a cofounder and board of directors member for Brahm Astra Therapeutics; and has intellectual property licensed to MDxHealth Inc., Aduro BioTech Inc., Clontech, Bristol Myers Squibb, and Brahm Astra Therapeutics.

https://doi.org/10.1016/j.ajpath.2022.09.010

metastatic spread has been documented in approximately 10% of men diagnosed with BCC.[4,9] The metastatic pattern of BCC is distinct, involving liver, lung, and bowel, but not bone, the most common site of acinar adenocarcinoma (AAC) of the prostate. These observations demonstrate that BCC clinically differs from AAC.[4]

From a molecular perspective, BCCs are characterized by the expression of prostatic basal cell markers, including p63 and high-molecular-weight keratins, and frequent overexpression of the antiapoptotic protein B-cell lymphoma 2 (BCL2).[10] Luminal prostate epithelial markers, including androgen receptor or prostate-specific antigen, are usually absent, or are expressed at low levels. In addition, BCCs do not harbor *TMPRSS2-ERG* gene rearrangements, which are seen in >50% of prostatic AACs.[11] Very little is known about the genomic features of BCC, and based on the small number of published studies, it appears that BCCs show limited copy number changes and rare recurrent translocations.[12,13]

To better characterize the genomic features of BCC, whole genome sequencing was performed on two BCC cases. Although the genomes of BCC are overall quiet, copy number loss of chromosome 16 was present in both cases. In addition, a loss of function mutation was observed in *CYLD*. In *in vitro* experiments, CYLD protein loss increased cell proliferation in prostatic basal cells, confirming its putative driver role. Furthermore, the loss of CYLD was associated with morphologic changes that resembled cylindromas, a skin tumor that arises in the context of familial cylindromatosis, which is characterized by *CYLD* inactivating mutations. Collectively this study provides further insights into the biology of BCCs and highlights the striking genotype-phenotype associations in tumors with *CYLD* alterations.

Materials and Methods

Patient Samples and Whole Genome Sequencing

Tissues consisted of archival transurethral resection specimens from the consultation files of one of the authors (J.I.E.). Tumor areas were identified by two pathologists (J.I.E. and M.C.H.) on adjacent hematoxylin and eosin–stained slides. These areas were macrodissected, and DNA was extracted from 5 formalin-fixed, paraffin-embedded tissue sections using a DNA formalin-fixed, paraffin-embedded tissue kit (QIAamp, Qiagen, Hilden, Germany) following manufacturer's protocols. Because of the fragmented nature of the transurethral resection specimens and the diffuse infiltrative growth pattern of the tumors, we aimed to achieve a tumor cellularity of >50%. In addition, adjacent, matched, non-neoplastic tissue was collected and used as germline control. DNA concentrations were determined using the a double-stranded DNA broad-range assay kit (Qubit, Invitrogen, Carlsbad, CA). Genomic DNA from tumor and adjacent benign samples was sonicated and further processed (TruSeq Nano DNA library construction kit, Illumina, San Diego, CA). Barcoded libraries were subjected to 151 × 151 paired end sequencing on a HiSeq 2500 Genome Analyzer (Illumina), resulting in a mean coverage of 28.9 (range, 29.5 to 27.22). Reads were aligned against the hg38 genome using the Burrows-Wheeler Alignment Tool version 0.7.7 with default setting.[14] Picard tools version 1.119 (Broad Institute, Cambridge, MA; *https://github.com/broadinstitute/picard*) were used to add read groups as well as remove duplicate reads. The Genome Analysis Toolkit version 3.6.0 (Broad Institute; *https://gatk.broadinstitute.org/hc/en-us*) base call recalibration steps were used to create the final alignment files.

Somatic Variant Detection

Somatic variants between the tumor-normal pairs were called using Mutect2 (Broad Institute) and Strelka2 (Illumina) and annotated with ANNOVAR.[15,16] Variants were further filtered for functional prediction evidence using the dbNSFP, and only deleterious variants supported by one of the prediction databases (SIFT, LRT, MutationTaster, and FATHMM) were considered. Variants were classified based on disease or phenotypes information using ClinVar, InterVar, and COSMIC. Synonymous and nonframeshift indels were excluded. Only variants supported by both callers (Mutect2 and Strelka2) were considered as final call sets.

Copy Number Analysis

Copy number analyses were performed using TitanCNA.[17,18] TitanCNA solutions were generated for one to three clonal clusters and ploidy initializations from two to four. Optimal solutions were selected automatically within the pipeline and reselected with manual inspection to confirm tumor ploidy and clonal cluster.

SV Analysis

SvABA and Gridss2 were used to detect structural variants (SVs). The SvABA analysis was performed using tumor-normal paired mode with default parameters.[19] SV events were classified into deletions, inversions, tandem duplications, interchromosomal translocations, and intrachromosomal translocations, whereas intrachromosomal translocations were further divided into balanced and unbalanced events based on copy number information as previously described.[20] Gene alteration status by genome rearrangements was defined based on the breakpoints of involved SV events. A gene in one whole genome sequencing sample (gene-sample pair) was considered to have gene-transecting events if any breakpoints of SV events were located within the gene body region. Gene coordinates were based on ENSEMBL version 33 (European Bioinformatics Institute, Hinxton, UK).[21] Circos plots were generated with shinyCircos

(YaoLab-Bioinfo, Guangzhou, China; *https://venyao.shinyapps.io/shinyCircos*).

In Vitro Experiments

Human telomerase reverse transcriptase (hTERT) immortalized prostate epithelial cells were a gift from John T. Isaacs (Johns Hopkins University, Baltimore, MD) and were grown in keratinocyte serum-free media (Thermo Fisher Scientific, Waltham, MA) supplemented with insulin, epidermal growth factor, and bovine pituitary extract (Thermo Fisher) as described previously.[22] *CYLD* shRNA sequences were obtained from The RNAi Consortium shRNA library (Broad Institute) and cloned into pLKO.1 backbones. Viral particles containing shRNA constructs were generated in HEK293T cells (ATCC, Manassas, VA) and transduced into cells. Seventy-two hours after transduction, cells were harvested for subsequent analyses. Western blot analysis was performed as described previously[23] with anti-CYLD (sc-74435, Santa Cruz Biotechnology, Dallas, TX) and anti−glyceraldehyde-3-phosphate dehydrogenase (ab8245, Abcam, Cambridge, UK) antibodies at 1:1000 and 1:10,000 dilutions, respectively. Cell growth assays were performed by seeding *CYLD* knock down and control cells on poly-L-lysine (Bio-Techne, Minneapolis, MN)−coated 96 well plates. Cell growth was monitored using a Biotek Cytation 5 live cell imager (Winooski, VT), and images were captured every 12 hours for a total of 4 days. Resulting images were analyzed using the Gen5 software version 3.10 (Biotek), and growth curves were plotted with GraphPad Prism software version 8 (GraphPad Inc., San Diego, CA).

Results

Histomorphologic assessment of case 1 showed nests of basaloid cells with a two-cell pattern and inner tubule formation characteristic of BCC. Cancer cells showed cytologic atypia and eosinophilic cytoplasm with an associated dense desmoplastic stromal reaction and an infiltrative growth pattern that involved 40% of the submitted specimen (Figure 1A). Whole genome sequencing revealed eight consensus protein-coding mutations; two variants in *DENND3* and *PTPRU* were previously described and included in the cosmic database (Figure 1B and Supplemental Table S1). In addition, this case showed a splice site mutation in exon 10 of *KIT* (Figure 1C and Supplemental Table S2). Shallow subclonal copy number loss of chromosomes 5, 13, and 14 and clonal hemizygous loss of the q-arm of chromosome 16 were noted (Figure 1C). There were 28 intrachromosomal SVs, including a complex rearrangement that involved the *ITGA2* gene on chromosome 5 (Supplemental Figure S1, Figure 2, and Supplemental Table S2).

Case 2 showed expansile tumor nests of variable size and shape with hyperchromatic nuclei at the periphery and larger pale cells in the center. The nests were aligned in a jigsaw pattern and were lined by a dense eosinophilic hyaline rim (Figure 2A). The tumor showed an invasive growth pattern that involved 10% of the submitted specimen with an elevated Ki-67 proliferation index (approximately 10%). A total of 10 protein-coding mutations were detected, which included stop gain mutations in *CYLD* and *GPR158* and a cosmic, annotated, nonsynonymous single-nucleotide variant in *MGA* (Figure 2B and Supplemental Table S1). Importantly, the *CYLD* alteration (Y710X) occurred in a region of hemizygous loss on chromosome 16 (Figure 2C and Supplemental Table S1). *CYLD* is a ubiquitously expressed putative tumor suppressor gene. Although the mutation seen in case 2 has not been previously described, it was predicted to result in a truncation of the ubiquitin carboxyl-terminal hydrolase domain, which is the core catalytic domain responsible for the deubiquitinase function of *CYLD*, therefore generating a catalytically dead enzyme (Supplemental Table S1). Copy number analyses showed an isolated copy number loss of chromosome 16 (Figure 2C). Three interchromosomal rearrangements were present, of which one directly involved the coding region of *ZNF407* (Supplemental Figure S2 and Supplemental Table S2).

hTERT immortalized prostate epithelial cells, which show basal cell features, were used to model the consequences of loss of *CYLD* function in prostatic basal cells.[22] Expression of a lentiviral shRNA construct targeting *CYLD* resulted in a robust depletion of CYLD protein levels (Figure 3A). To determine the changes in cell proliferation on *CYLD* knock down, live cell imaging of short hairpin *CYLD* and short hairpin control expressing cells was performed. Compared with short hairpin control-transduced cells, *CYLD*-depleted cells showed a significant increase in cell proliferation (Figure 3B). These data suggest that loss of CYLD can promote basal cell proliferation and validate the functional significance of *CYLD* loss as seen in case 2.

Discussion

Prostatic BCCs are rare tumors of the prostate that, as opposed to the much more common AAC, demonstate features of basal cell differentiation. Prior studies suggested that BCCs have a different genomic makeup compared with AACs. However, to date, comprehensive whole genome sequencing studies have not been performed on BCCs. The genomic features of AAC of the prostate have been extensively characterized during the past decade, and key driver gene alterations that involve mutations in *TP53*, *SPOP*, *FOXA1,* and *PTEN* as well as recurrent rearrangements that involve Ets transcription factors and frequent copy number changes have been described.[24–27]

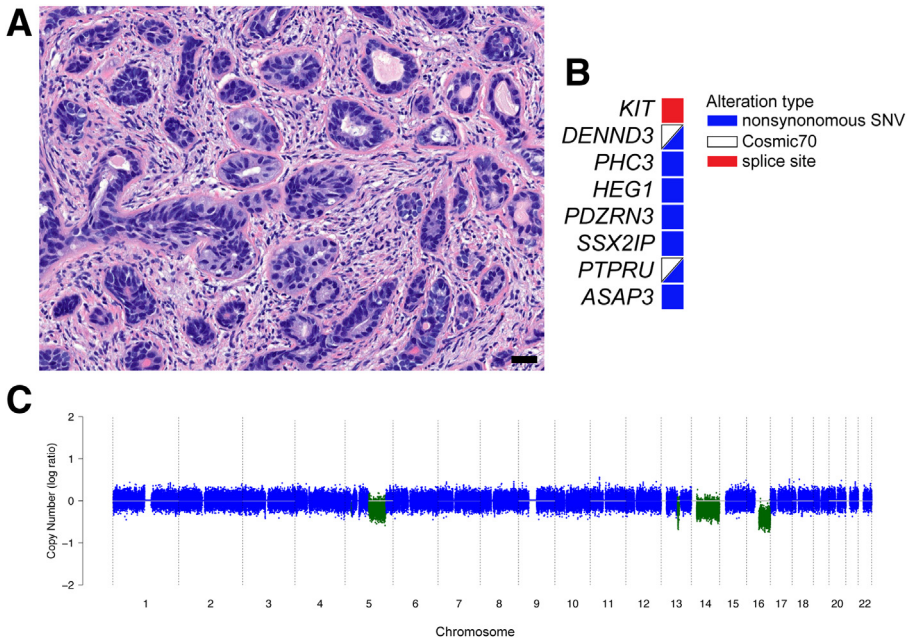

Figure 1 **A:** Hematoxylin and eosin–stained micrograph showing histomorphologic features of case 1. Note the nuclear atypia and dense desmoplastic response in this case. **B:** Table listing consensus single-nucleotide variants as well as insertions and deletions. **C:** Copy number profile highlights copy number losses (green) that affect chromosomes 5, 13, 14, and 16. Dots represent normalized log ratios for 10-kb windows. Blue indicates copy neutral; green, copy number loss. Scale bar = 50 μm (**A**).

Herein, the first whole genome sequencing study of this rare tumor type was performed to gain insights into the spectrum of genomic changes in BCCs. An overall low rate of single-nucleotide variants, SVs, and copy number changes was observed in the two tumors analyzed. Notably, none of the genomic alterations commonly found in AACs were identified, demonstrating that BCCs are indeed genomically distinct from AACs (Supplemental Figure S3).[28,29]

Case 1 showed a splice site mutation in *KIT* with predicted high functional impact as well as mutations in

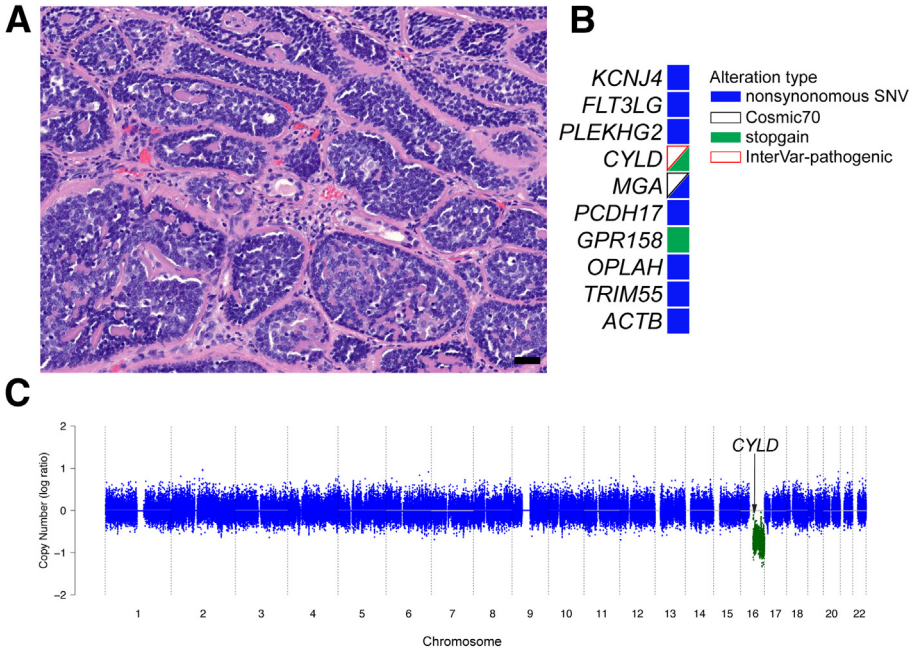

Figure 2 **A:** Hematoxylin and eosin–stained micrograph showing histomorphologic features of case 2. Note the cribriform-like growth pattern with abundant eosinophilic basement membrane material that resembles cylindromas of the skin. **B:** Table listing consensus single-nucleotide variants (SNVs) and insertions and deletions. **C:** Copy number profile highlights copy number loss (green) affecting chromosome 16. Dots represent normalized log ratios for 10-kb windows. Blue indicates copy neutral; green, copy number loss. Scale bar = 50 μm (**A**).

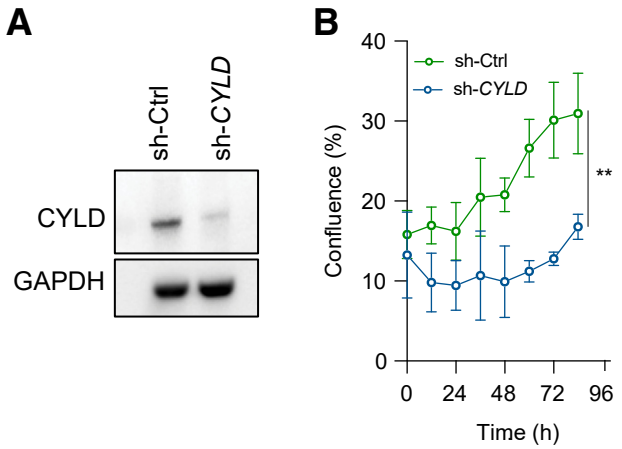

Figure 3 **A:** Western blot analysis of benign basal-like prostate epithelial cells stably transduced with nontargeting control vectors [short hairpin control (sh-Ctrl)] and *CYLD* targeting shRNAs [short hairpin *CYLD* (sh-*CYLD*)] demonstrate effective depletion of CYLD protein levels. **B:** Cell proliferation assessment based on cellular confluency determined by live cell imaging of sh-*CYLD* and sh-Ctrl cells. $*P < 0.01$. GAPDH, glyceraldehyde-3-phosphate dehydrogenase.

DENND3 and *PTPRU*. Genomic alterations of *KIT* are commonly found in gastrointestinal stroma tumors, seminoma, and acute myeloid leukemia.[30–32] Activating missense mutations in the kinase domain are the most common somatic alteration in cancer, but recurrent splice site changes have also been described.[33,34] Although the significance of this mutation in this case is unclear, its enrichment in gastrointestinal stroma tumors, which are known to be driven by genomic alterations in *KIT,* suggests a potential driver function. However, the fact that the *KIT* mutation seen here is upstream of the kinase domain and that most gastrointestinal stroma tumors harboring this alteration also showed other *KIT* mutations complicates the assessment of the potential functional consequence.[34] *PTPRU* is part of the R2B receptors and was reported to play a role in gastric cancer and glioma.[35,36] *DENND3* belongs to the DENN domain–containing protein family of Rab guanine nucleotide exchange factors, which have been shown to be involved in the pathogenesis of familial frontotemporal dementia and amyotrophic lateral sclerosis.[37–39] In addition, case 1 showed several large-scale copy number losses, including a hemizygous loss of chromosome 16q that involved the *CYLD* locus, but no single-nucleotide alterations in the *CYLD* gene were observed.

Case 2 had mutations in *MGA* and *GPR158*. MAX gene-associated (MGA) protein was shown to bind MYC associated factor X (MAX), which is a critical molecule that dimerizes with MYC oncogenic transcription factors.[40,41] Ectopic expression of MGA suppresses growth of lung adenocarcinoma cell lines.[42] Conversely, *MGA* loss promotes lung tumorigenesis *in vivo* and human colon cancer growth in organoids models.[43] The orphan receptor GPR158 is up-regulated in metastatic castration resistant prostate cancer and is thought to promote growth and invasion.[44]

Although recent studies have demonstrated recurrent translocations encompassing the *MYB* oncogene in prostatic BCC, these translocations were not present in the two cases studied here.[45,46] The t(6;9)(q22-23;p23-24) translocation resulting in the *MYB-NFIB* fusion protein are commonly found in adenoid cystic carcinoma of the salivary gland, and similar *MYB* gene rearrangements were detectable in 2/12 adenoid cystic carcinoma–like BCCs but in none of the BCCs with a solid growth pattern.[45,47] The tight association between *MYB* gene alterations and adenoid cystic morphology suggests that certain driver gene alterations can result in histomorphologic features common across different tumor types.

It is worth noting that a somatic stop gain mutation in *CYLD* with associated copy number loss was observed in case 2. Germline *CYLD* mutations are associated with familial cylindromatosis, a rare inherited skin tumor syndrome, in which patients have multiple cylindromas.[48–50] Although cylindromas share histologic similarities with adenoid cystic carcinoma, they are characterized by islands of basaloid cells often arranged in a jigsaw pattern separated from the stroma by a thickened basement membrane.[48,51] The morphologic features characteristic of cylindromas are remarkably similar to the histomorphologic appearance of case 2. The truncating stop gain mutation in *CYLD* observed in case 2 is located upstream of the ubiquitin carboxyl-terminal hydrolase domain. Therefore, the resulting protein lacks catalytic activity. CYLD negatively regulates NF-κB, WNT, and JNK signaling, and inactivating mutations can result in aberrant pathway activation, ultimately leading to enhanced cell proliferation, inhibition of apoptosis, and increased cell migration in epidermal cell systems.[52–56] To study the biological consequences of the loss of function alteration in *CYLD*, shRNA was used to knock down CYLD expression. *CYLD* depletion resulted in significantly increased cell proliferation. Collectively, these observations suggest that herein, the observed *CYLD* mutation is likely a driver gene alteration.

In both human and murine prostates, the basal cell compartment harbors stem cells that can contribute to the regeneration of benign prostate epithelia.[57] Transformation of isolated prostatic basal cells with oncogenic drivers commonly found in acinar prostate cancer results in tumors with a luminal cell phenotype.[58,59] However, different basal cell populations have different propensities to form tumors with a luminal cell phenotype.[59] It is therefore possible that subsets of prostatic basal cells with distinct molecular characteristics are capable of giving rise to a prostatic BCC. Alternatively, given the differences in genomic driver alterations observed between AACs and BCCs, the composition of oncogenic drivers, rather than the cell of origin, could determine the lineage phenotype of the tumor.

In summary, this study provides novel insights into the biology of prostatic BCC, highlights potential driver gene

alterations, and emphasizes the genotype-morphologic phenotype correlation associated with certain driver gene alterations across different cell lineages.

Acknowledgment

We thank the Sidney Kimmel Comprehensive Cancer Center Experimental and Computational Genomics Core at Johns Hopkins for assistance with the whole genome sequencing studies.

Supplemental Data

Supplemental material for this article can be found at *http://doi.org/10.1016/j.ajpath.2022.09.010*.

References

1. Zhang D, Zhao S, Li X, Kirk JS, Tang DG: Prostate luminal progenitor cells in development and cancer. Trends Cancer 2018, 4: 769−783
2. Humphrey PA: Histopathology of prostate cancer. Cold Spring Harb Perspect Med 2017, 7:a030411
3. Ali TZ, Epstein JI: Basal cell carcinoma of the prostate: a clinicopathologic study of 29 cases. Am J Surg Pathol 2007, 31:697−705
4. Iczkowski KA, Ferguson KL, Grier DD, Hossain D, Banerjee SS, McNeal JE, Bostwick DG: Adenoid cystic/basal cell carcinoma of the prostate: clinicopathologic findings in 19 cases. Am J Surg Pathol 2003, 27:1523−1529
5. McKenney JK, Amin MB, Srigley JR, Jimenez RE, Ro JY, Grignon DJ, Young RH: Basal cell proliferations of the prostate other than usual basal cell hyperplasia: a clinicopathologic study of 23 cases, including four carcinomas, with a proposed classification. Am J Surg Pathol 2004, 28:1289−1298
6. Grignon DJ, Ro JY, Ordoñez NG, Ayala AG, Cleary KR: Basal cell hyperplasia, adenoid basal cell tumor, and adenoid cystic carcinoma of the prostate gland: an immunohistochemical study. Hum Pathol 1988, 19:1425−1433
7. Ayyathurai R, Civantos F, Soloway MS, Manoharan M: Basal cell carcinoma of the prostate: current concepts. BJU Int 2007, 99: 1345−1349
8. Thorson P, Swanson PE, Vollmer RT, Humphrey PA: Basal cell hyperplasia in the peripheral zone of the prostate. Mod Pathol 2003, 16:598−606
9. Tsuruta K, Funahashi Y, Kato M: Basal cell carcinoma arising in the prostate. Int J Urol 2014, 21:1072−1073
10. Yang XJ, McEntee M, Epstein JI: Distinction of basaloid carcinoma of the prostate from benign basal cell lesions by using immunohistochemistry for bcl-2 and Ki-67. Hum Pathol 1998, 29:1447−1450
11. Weier C, Haffner MC, Mosbruger T, Esopi DM, Hicks J, Zheng Q, Fedor H, Isaacs WB, De Marzo AM, Nelson WG, Yegnasubramanian S: Nucleotide resolution analysis of TMPRSS2and ERG rearrangements in prostate cancer. J Pathol 2013, 230:174−183
12. Luebke AM, Schlomm T, Gunawan B, Bonkhoff H, Füzesi L, Erbersdobler A: Simultaneous tumour-like, atypical basal cell hyperplasia and acinar adenocarcinoma of the prostate: a comparative morphological and genetic approach. Virchows Arch 2005, 446: 338−341
13. Su X, Long Q, Bo J, Shi Y, Zhao L-N, Lin Y, Luo Q, Ghazanfar S, Zhang C, Liu Q, Wang L, He K, He J, Cui X, Yang JYH, Han Z-G, Yang G, Sha J-J: Mutational and transcriptomic landscapes of a rare human prostate basal cell carcinoma. Prostate 2020, 80:508−517
14. Li H, Durbin R: Fast and accurate short read alignment with Burrows-Wheeler transform. Bioinformatics 2009, 25:1754−1760
15. DePristo MA, Banks E, Poplin R, Garimella KV, Maguire JR, Hartl C, Philippakis AA, del Angel G, Rivas MA, Hanna M, McKenna A, Fennell TJ, Kernytsky AM, Sivachenko AY, Cibulskis K, Gabriel SB, Altshuler D, Daly MJ: A framework for variation discovery and genotyping using next-generation DNA sequencing data. Nat Genet 2011, 43:491−498
16. Kim S, Scheffler K, Halpern AL, Bekritsky MA, Noh E, Källberg M, Chen X, Kim Y, Beyter D, Krusche P, Saunders CT: Strelka2: fast and accurate calling of germline and somatic variants. Nat Methods 2018, 15:591−594
17. Ha G, Roth A, Khattra J, Ho J, Yap D, Prentice LM, Melnyk N, McPherson A, Bashashati A, Laks E, Biele J, Ding J, Le A, Rosner J, Shumansky K, Marra MA, Gilks CB, Huntsman DG, McAlpine JN, Aparicio S, Shah SP: TITAN: inference of copy number architectures in clonal cell populations from tumor whole-genome sequence data. Genome Res 2014, 24:1881−1893
18. Adalsteinsson VA, Ha G, Freeman SS, Choudhury AD, Stover DG, Parsons HA, et al: Scalable whole-exome sequencing of cell-free DNA reveals high concordance with metastatic tumors. Nat Commun 2017, 8:1324
19. Wala JA, Bandopadhayay P, Greenwald NF, O'Rourke R, Sharpe T, Stewart C, Schumacher S, Li Y, Weischenfeldt J, Yao X, Nusbaum C, Campbell P, Getz G, Meyerson M, Zhang C-Z, Imielinski M, Beroukhim R: SvABA: genome-wide detection of structural variants and indels by local assembly. Genome Res 2018, 28:581−591
20. Viswanathan SR, Ha G, Hoff AM, Wala JA, Carrot-Zhang J, Whelan CW, Haradhvala NJ, Freeman SS, Reed SC, Rhoades J, Polak P, Cipicchio M, Wankowicz SA, Wong A, Kamath T, Zhang Z, Gydush GJ, Rotem D; PCF/SU2C International Prostate Cancer Dream Team, Love JC, Getz G, Gabriel S, Zhang C-Z, Dehm SM, Nelson PS, Van Allen EM, Choudhury AD, Adalsteinsson VA, Beroukhim R, Taplin M-E, Meyerson M: Structural alterations driving castration-resistant prostate cancer revealed by linked-read genome sequencing. Cell 2018, 174:433−447.e19
21. Howe KL, Achuthan P, Allen J, Allen J, Alvarez-Jarreta J, Amode MR, et al: Ensembl 2021. Nucleic Acids Res 2021, 49: D884−D891
22. Graham MK, Principessa L, Antony L, Meeker AK, Isaacs JT: Low p16INK4a expression in early passage human prostate basal epithelial cells enables immortalization by telomerase expression alone. Prostate 2017, 77:374−384
23. Haffner MC, Aryee MJ, Toubaji A, Esopi DM, Albadine R, Gurel B, Isaacs WB, Bova GS, Liu W, Xu J, Meeker AK, Netto G, De Marzo AM, Nelson WG, Yegnasubramanian S: Androgen-induced TOP2B-mediated double-strand breaks and prostate cancer gene rearrangements. Nat Genet 2010, 42:668−675
24. Armenia J, Wankowicz SAM, Liu D, Gao J, Kundra R, Reznik E, et al: The long tail of oncogenic drivers in prostate cancer. Nat Genet 2018, 50:645−651
25. Robinson D, Van Allen EM, Wu Y-M, Schultz N, Lonigro RJ, Mosquera J-M, et al: Integrative clinical genomics of advanced prostate cancer. Cell 2015, 161:1215−1228
26. Wedge DC, Gundem G, Mitchell T, Woodcock DJ, Martincorena I, Ghori M, et al: Sequencing of prostate cancers identifies new cancer genes, routes of progression and drug targets. Nat Genet 2018, 50: 682−692
27. Cancer Genome Atlas Research Network: The molecular taxonomy of primary prostate cancer. Cell 2015, 163:1011−1025
28. Cerami E, Gao J, Dogrusoz U, Gross BE, Sumer SO, Aksoy BA, Jacobsen A, Byrne CJ, Heuer ML, Larsson E, Antipin Y, Reva B, Goldberg AP, Sander C, Schultz N: The cBio cancer genomics portal: an open platform for exploring multidimensional cancer genomics data. Cancer Discov 2012, 2:401−404

29. Gao J, Aksoy BA, Dogrusoz U, Dresdner G, Gross B, Sumer SO, Sun Y, Jacobsen A, Sinha R, Larsson E, Cerami E, Sander C, Schultz N: Integrative analysis of complex cancer genomics and clinical profiles using the cBioPortal. Sci Signal 2013, 6:pl1
30. Corless CL, Barnett CM, Heinrich MC: Gastrointestinal stromal tumours: origin and molecular oncology. Nat Rev Cancer 2011, 11: 865−878
31. Coombs CC, Tallman MS, Levine RL: Molecular therapy for acute myeloid leukaemia. Nat Rev Clin Oncol 2016, 13:305−318
32. Litchfield K, Levy M, Huddart RA, Shipley J, Turnbull C: The genomic landscape of testicular germ cell tumours: from susceptibility to treatment. Nat Rev Urol 2016, 13:409−419
33. Heinrich MC, Rubin BP, Longley BJ, Fletcher JA: Biology and genetic aspects of gastrointestinal stromal tumors: KIT activation and cytogenetic alterations. Hum Pathol 2002, 33:484−495
34. Chen LL, Sabripour M, Wu EF, Prieto VG, Fuller GN, Frazier ML: A mutation-created novel intra-exonic pre-mRNA splice site causes constitutive activation of KIT in human gastrointestinal stromal tumors. Oncogene 2005, 24:4271−4280
35. Zhu Z, Liu Y, Li K, Liu J, Wang H, Sun B, Xiong Z, Jiang H, Zheng J, Hu Z: Protein tyrosine phosphatase receptor U (PTPRU) is required for glioma growth and motility. Carcinogenesis 2014, 35: 1901−1910
36. Liu Y, Zhu Z, Xiong Z, Zheng J, Hu Z, Qiu J: Knockdown of protein tyrosine phosphatase receptor U inhibits growth and motility of gastric cancer cells. Int J Clin Exp Pathol 2014, 7:5750−5761
37. Renton AE, Majounie E, Waite A, Simón-Sánchez J, Rollinson S, Gibbs JR, et al: A hexanucleotide repeat expansion in C9ORF72 is the cause of chromosome 9p21-linked ALS-FTD. Neuron 2011, 72: 257−268
38. Nickerson ML, Warren MB, Toro JR, Matrosova V, Glenn G, Turner ML, Duray P, Merino M, Choyke P, Pavlovich CP, Sharma N, Walther M, Munroe D, Hill R, Maher E, Greenberg C, Lerman MI, Linehan WM, Zbar B, Schmidt LS: Mutations in a novel gene lead to kidney tumors, lung wall defects, and benign tumors of the hair follicle in patients with the Birt-Hogg-Dubé syndrome. Cancer Cell 2002, 2:157−164
39. Xu J, McPherson PS: Regulation of DENND3, the exchange factor for the small GTPase Rab12 through an intramolecular interaction. J Biol Chem 2017, 292:7274−7282
40. Hurlin PJ, Steingrìmsson E, Copeland NG, Jenkins NA, Eisenman RN: Mga, a dual-specificity transcription factor that interacts with Max and contains a T-domain DNA-binding motif. EMBO J 1999, 18:7019−7028
41. Amati B, Brooks MW, Levy N, Littlewood TD, Evan GI, Land H: Oncogenic activity of the c-Myc protein requires dimerization with Max. Cell 1993, 72:233−245
42. Llabata P, Mitsuishi Y, Choi PS, Cai D, Francis JM, Torres-Diz M, Udeshi ND, Golomb L, Wu Z, Zhou J, Svinkina T, Aguilera-Jimenez E, Liu Y, Carr SA, Sanchez-Cespedes M, Meyerson M, Zhang X: Multi-omics analysis identifies MGA as a negative regulator of the MYC pathway in lung adenocarcinoma. Mol Cancer Res 2020, 18:574−584
43. Mathsyaraja H, Catchpole J, Freie B, Eastwood E, Babaeva E, Geuenich M, Cheng PF, Ayers J, Yu M, Wu N, Moorthi S, Poudel KR, Koehne A, Grady W, Houghton AM, Berger AH, Shiio Y, MacPherson D, Eisenman RN: Loss of MGA repression mediated by an atypical polycomb complex promotes tumor progression and invasiveness. Elife 2021, 10:e64212
44. Patel N, Itakura T, Jeong S, Liao C-P, Roy-Burman P, Zandi E, Groshen S, Pinski J, Coetzee GA, Gross ME, Fini ME: Expression and functional role of orphan receptor GPR158 in prostate cancer growth and progression. PLoS One 2015, 10:e0117758
45. Bishop JA, Yonescu R, Epstein JI, Westra WH: A subset of prostatic basal cell carcinomas harbor the MYB rearrangement of adenoid cystic carcinoma. Hum Pathol 2015, 46:1204−1208
46. Magers MJ, Iczkowski KA, Montironi R, Grignon DJ, Zhang S, Williamson SR, Yang X, Wang M, Osunkoya AO, Lopez-Beltran A, Hes O, Eble JN, Cheng L: MYB-NFIB gene fusion in prostatic basal cell carcinoma: clinicopathologic correlates and comparison with basal cell adenoma and florid basal cell hyperplasia. Mod Pathol 2019, 32:1666−1674
47. Rettig EM, Talbot CC, Sausen M, Jones S, Bishop JA, Wood LD, Tokheim C, Niknafs N, Karchin R, Fertig EJ, Wheelan SJ, Marchionni L, Considine M, Ling S, Fakhry C, Papadopoulos N, Kinzler KW, Vogelstein B, Ha PK, Agrawal N: Whole-genome sequencing of salivary gland adenoid cystic carcinoma. Cancer Prev Res 2016, 9:265−274
48. Rajan N, Ashworth A: Inherited cylindromas: lessons from a rare tumour. Lancet Oncol 2015, 16:e460−e469
49. Verhoeft KR, Ngan HL, Lui VWY: The cylindromatosis (CYLD) gene and head and neck tumorigenesis. Cancers Head Neck 2016, 1: 10−16
50. Singh DD, Naujoks C, Depprich R, Schulte K-W, Jankowiak F, Kübler NR, Handschel J: Cylindroma of head and neck: review of the literature and report of two rare cases. J Craniomaxillofac Surg 2013, 41:516−521
51. Bignell GR, Warren W, Seal S, Takahashi M, Rapley E, Barfoot R, Green H, Brown C, Biggs PJ, Lakhani SR, Jones C, Hansen J, Blair E, Hofmann B, Siebert R, Turner G, Evans DG, Schrander-Stumpel C, Beemer FA, van Den Ouweland A, Halley D, Delpech B, Cleveland MG, Leigh I, Leisti J, Rasmussen S: Identification of the familial cylindromatosis tumour-suppressor gene. Nat Genet 2000, 25:160−165
52. Alameda JP, Moreno-Maldonado R, Navarro M, Bravo A, Ramírez A, Page A, Jorcano JL, Fernández-Aceñero MJ, Casanova ML: An inactivating CYLD mutation promotes skin tumor progression by conferring enhanced proliferative, survival and angiogenic properties to epidermal cancer cells. Oncogene 2010, 29:6522−6532
53. Brummelkamp TR, Nijman SMB, Dirac AMG, Bernards R: Loss of the cylindromatosis tumour suppressor inhibits apoptosis by activating NF-kappaB. Nature 2003, 424:797−801
54. Lee CC, Carette JE, Brummelkamp TR, Ploegh HL: A reporter screen in a human haploid cell line identifies CYLD as a constitutive inhibitor of NF-κB. PLoS One 2013, 8:e70339
55. Reiley W, Zhang M, Sun S-C: Negative regulation of JNK signaling by the tumor suppressor CYLD. J Biol Chem 2004, 279:55161−55167
56. Kovalenko A, Chable-Bessia C, Cantarella G, Israël A, Wallach D, Courtois G: The tumour suppressor CYLD negatively regulates NF-kappaB signalling by deubiquitination. Nature 2003, 424:801−805
57. De Marzo AM, Meeker AK, Epstein JI, Coffey DS: Prostate stem cell compartments: expression of the cell cycle inhibitor p27Kip1 in normal, hyperplastic, and neoplastic cells. Am J Pathol 1998, 153: 911−919
58. Goldstein AS, Huang J, Guo C, Garraway IP, Witte ON: Identification of a cell of origin for human prostate cancer. Science 2010, 329: 568−571
59. Stoyanova T, Cooper AR, Drake JM, Liu X, Armstrong AJ, Pienta KJ, Zhang H, Kohn DB, Huang J, Witte ON, Goldstein AS: Prostate cancer originating in basal cells progresses to adenocarcinoma propagated by luminal-like cells. Proc Natl Acad Sci U S A 2013, 110:20111−20116